REPRESENTATION OF THE GEOSYNCHRONOUS PLASMA ENVIRONMENT FOR SPACECRAFT CHARGING CALCULATIONS

V. A. Davis
Science Applications International Corporation
10260 Campus Point Dr., M.S. A1
San Diego, CA, 92121
Phone: 858-826-1608
Fax: 858-826-1652
E-mail: victoria.a.davis@saic.com

M. J. Mandell
Science Applications International Corporation

M. F. Thomsen
Los Alamos National Laboratory

Historically, our ability to predict and "postdict" surface charging has suffered from both a lack of reliable secondary emission and backscattered electron yields and poor characterization of the plasma environment. One difficulty lies in the common practice of fitting the plasma data to a Maxwellian or Double Maxwellian distribution function, which may not represent the data well for charging purposes.

For 13 years Los Alamos National Laboratory (LANL) has been accumulating measurements of electron and proton spectra from Magnetospheric Plasma Analyzer (MPA) instruments aboard a series of geosynchronous satellites. These data provide both a plasma characterization and the potential of the instrument ground.

We use electron and ion flux spectra measured by the LANL MPA to examine how the use of different spectral representations of the charged particle environment in computations of spacecraft potentials during magnetospheric substorms affects the accuracy of the results. We calculate the spacecraft potential using both the measured fluxes and several different fits to these fluxes. These flux measurements and fits have been corrected for the difference between the measured and calculated potential. The potentials computed using the measured fluxes, the best available material properties of graphite carbon, and a secondary electron escape fraction of 81%, are within a factor of three of the measured potential for nearly all the data. Using a Kappa fit to the electron distribution function and a Maxwellian fit to the ion distribution function gives agreement similar to the calculations using the actual data. Alternative spectral representations, including Maxwellian and double Maxwellian for both species, lead to less satisfactory agreement between predicted and measured potentials.

Background

Historically, our ability to predict and "postdict" spacecraft surface charging has suffered from both a lack of reliable secondary emission and backscattered electron yields and poor characterization of the plasma environment. One difficulty lies in the common practice of fitting

the plasma data to a Maxwellian or Double Maxwellian distribution function, which may not represent the data well for charging purposes. We examine how the use of different spectral representations of the charged particle environment in computations of spacecraft potentials during magnetospheric substorms affects the accuracy of the calculations.

The approach is as follows:

1. Examine charging and non-charging, electron and ion fluxes to determine relevant spectral characteristics.
2. Compute net fluxes and correlate with potential.
3. Compare the measured potential with the potential computed from measured fluxes to validate the charging computation.
4. Determine the analytic representation that best preserves the charging characteristics.

Data

For 13 years Los Alamos National Laboratory (LANL) has been accumulating measurements of electron and proton spectra from Magnetospheric Plasma Analyzer (MPA) instruments aboard a series of geosynchronous satellites.[1] The MPA is a spherical section electrostatic analyzer. The MPA is mounted so that the spacecraft spin allows the instrument to view 360° in azimuth. These data provide both a plasma characterization and the potential of the instrument ground.[2] We use electron and ion spectra measured by the LANL MPA and compare predictions with observed charging potentials. We focus on data taken by one MPA during eclipse periods in September 2001. This dataset has 973 measurements of charging to potentials ranging from 3 V to nearly 10 kV negative.

Fluxes

In eclipse, the net charging flux to the spacecraft is the sum of the incident electron and ion fluxes and secondary and backscattered electron fluxes.[3] The integral of the incident spectrum against the area-averaged yield functions gives the secondary and backscattered fluxes. Steady-state is established when the net charging flux is zero.

For a spacecraft charged to a surface potential of ϕ, the net charging flux can be written as the difference between the net ion and electron fluxes, given by the following expressions:

$$\text{Flux}_{\text{net}}^{\text{e}} = \int_{0}^{\infty} F_e(E)\left[1 - \gamma Y_e(E) - B(E)\right]dE = \sum_{E > E_{\text{min}}} F_e(E)\left(1 - \gamma Y_e(E) - B(E)\right)\Delta E \quad (1)$$

$$\text{Flux}_{\text{net}}^{\text{i}} = \int_{-\phi}^{\infty} F_i(E)\left[1 + \gamma Y_i(E)\right]dE = \sum_{E} F_i(E)\left(1 + \gamma Y_i(E)\right)\Delta E$$

F_e and F_i are the measured electron and ion fluxes respectively, the Y_e and Y_i are the area-averaged secondary yields due to electron and ion flux respectively, B is the area-averaged backscattered yield, and γ is the fraction of low-energy electrons that escape. The electron

minimum energy, E_{min}, used is the minimum of $-\phi/2$ and 30 eV. Many of the low-energy secondary electrons are trapped by electric fields due to differential potentials. The value of E_{min} is selected to remove these secondaries from the integral, while including some of the structure of the low energy portion of the spectrum in the non and low charging cases.

If we use graphite material properties to represent the area-averaged material and assume that all the secondary electrons escape, the measured potential as a function of the measured incident electron flux and the net electron flux, calculated according to Equation 1, appears as shown in Figure 1. This figure illustrates the difficulties of assuming that the potential is a function of either the incident electron flux or the net electron flux alone. While from the figure one could argue that there is a correlation between the potential and the average net electron flux, the net electron flux value does not provide a good prediction of the potential.
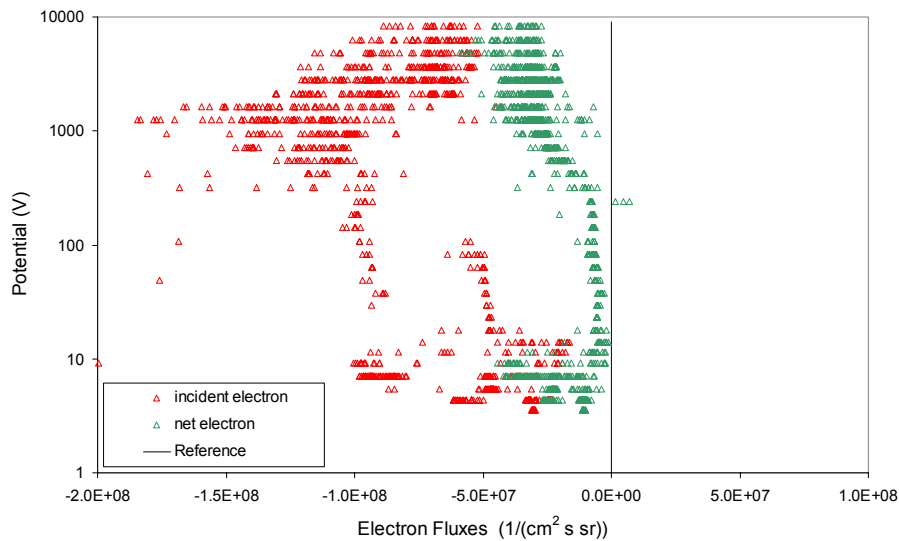
Figure 1. Incident and net electron fluxes at all potentials. The quantity plotted is minus the flux.

The net electron and ion fluxes, computed under the above assumptions, appear in Figure 2. If the material properties were perfectly known and the spectrum perfectly measured, the sum of the net electron and ion fluxes, the net charging flux, would be zero. As, on the average, the net charging flux is about 10% of the incident electron flux and greater than the incident ion flux, these properties provide poor potential estimates. We also computed the net charging flux using different techniques to compute the integral and different strategies to compute E_{min}. The results do not vary significantly. We computed the net charging flux using the material properties of gold, Kapton, solar cells, and optical solar reflectors for all of the materials and got much larger net charging fluxes. However, as shown in Figure 3, the net charging flux computed using the properties of graphite can be made to fall near zero for most of the data, if a value of 0.81 for γ is assumed.
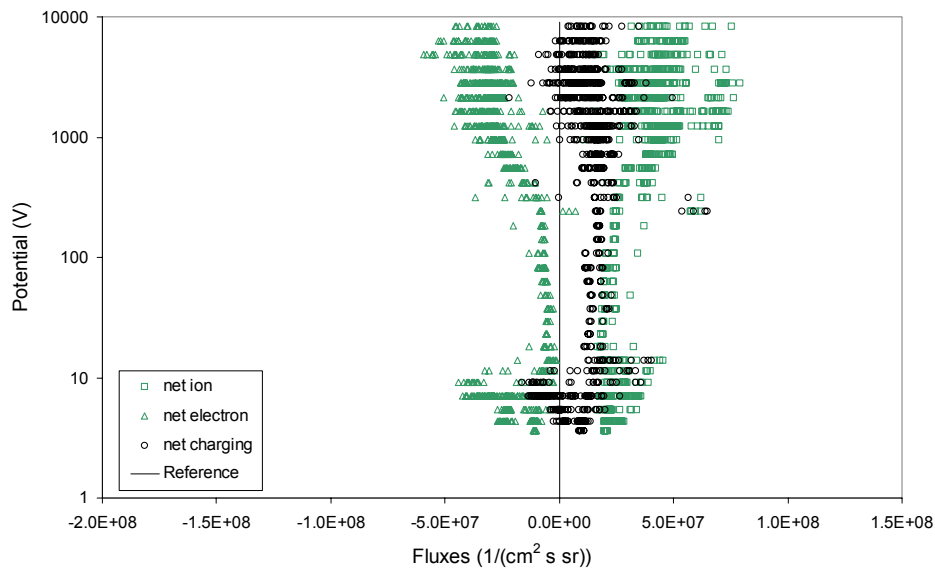
Figure 2. Net ion and electron fluxes and their difference, the net charging flux. For the net electron flux, the quantity plotted is minus the flux. A complete flux spectrum, correct yield function, and proper accounting for suppression of secondaries by barriers would give a value of zero for all potentials.

Figure 3. Net electron and ion fluxes and their sum, the net charging flux, assuming that only 81% of the electrons escape. For the net electron flux, the quantity plotted is minus the flux.

Potential Computation

The approach for the potential calculation using measured fluxes is as follows:

1. Given the measured potential, use the measured spectra and Liouville's theorem to compute the ion and electron spectra at infinity.

2. Using the computed ion and electron spectra at infinity, determine the net charging flux (incident, secondaries, and backscattered) to the spacecraft as a function of the spacecraft chassis potential.

3. Search for a unique chassis potential between -1 V and -10,000 V at which the net charging flux magnitude is zero, or a minimum.

4. If the computed and measured potential are within experimental error of each other, the potential prediction technique is good.

The net charging flux in terms of the measured fluxes, F_e and F_i, the proposed potential, ϕ', and the measured potential, ϕ_m, is given by

$$F_{net}(\phi') = - \int_{max(0,\phi_m-\phi')}^{\infty} dE_m \left(1 - \frac{\phi_m - \phi'}{E_m}\right) F_e(E_m)\left[1 - \gamma(\phi')Y_e(E_m - \phi_m + \phi') - B(E_m - \phi_m + \phi')\right]$$

$$+ \int_{-\phi_m}^{\infty} dE_m \left(1 + \frac{\phi_m - \phi'}{E_m}\right) F_i(E_m)\left[1 + \gamma(\phi')Y_i(E_m + \phi_m - \phi')\right] \qquad (2)$$

Figure 4 shows the potential computed using the measured fluxes and the best available material properties of graphite carbon, with a secondary electron escape fraction of 81%. The computed potential is within a factor of 1.5 of the measured potential for 66% of the data and within a factor of 3 for 87% of the data.

81% low energy electrons escape

Eclipse; 81% escape
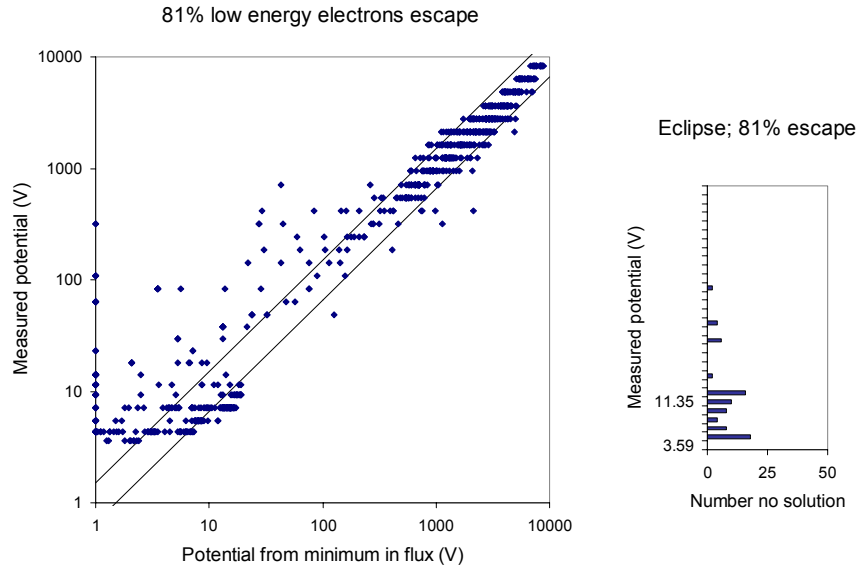
Figure 4. Meaured potential as a function of the potential computed from the minimum in the net charging flux with 81% escape fraction.

Potentials Using Fit Fluxes

The potentials can be computed using a fit to the measured fluxes as well as using the measured fluxes themselves. Several functions were tried. Those that work best are the traditional Maxwellian and double Maxwellian and the Kappa distribution. The Kappa distribution was selected for investigation as Christon, *et al*[4] have shown that it provides a good fit to the quiescent plasma sheet environment at greater than 12 R_E. (Geosynchronous is at 6.6 R_E.) The Kappa function has the shape of a Maxwellian at low energies and a power law at high energies, providing a high-energy tail to the distribution.

$$\mathrm{Flux}^{\mathrm{Maxwellian}}\left(E\right) = n\frac{e}{4\pi}\sqrt{\frac{1}{2\pi m e \theta}}\frac{E}{\theta}\exp\left(-\frac{E}{\theta}\right)$$

$$\mathrm{Flux}^{\mathrm{DoubleMaxwellian}}\left(E\right) = en_1\sqrt{\frac{1}{2\pi m e \theta_1}}\frac{E}{\theta_1}\exp\left(-\frac{E}{\theta_1}\right) + en_2\sqrt{\frac{1}{2\pi m e \theta_2}}\frac{E}{\theta_2}\exp\left(-\frac{E}{\theta_2}\right) \quad (3)$$

$$\mathrm{Flux}^{\mathrm{Kappa}}\left(E\right) = A\,E\left(1+\frac{E}{\kappa E_o}\right)^{-\kappa-1}$$

The most accurate potential predictions, shown in Figure 5, were obtained using a Kappa function fit to the electron distribution and a Maxwellian function fit to the ion distribution. The potentials computed using the fit agree with the measured potentials about as well as the potentials computed using the measured fluxes directly. The computed potential is within a factor of 1.5 of the measured potential for 65% of the data and within a factor of 3 for 80% of the data. Alternative spectral representations, including Maxwellian or Kappa distributions for both species, led to less satisfactory agreement between predicted and measured potentials.

The Kappa-Maxwellian fits often generate no potential solution between 30 and 300 V and sometimes predict high potentials for low measured-potential cases. These high-predicted potentials were examined. The automated fitting of the low temperature ion spectrum gives a high temperature Maxwellian due to the high weight of the wider higher potential bins. A smarter fitting procedure would give more accurate potential predictions.
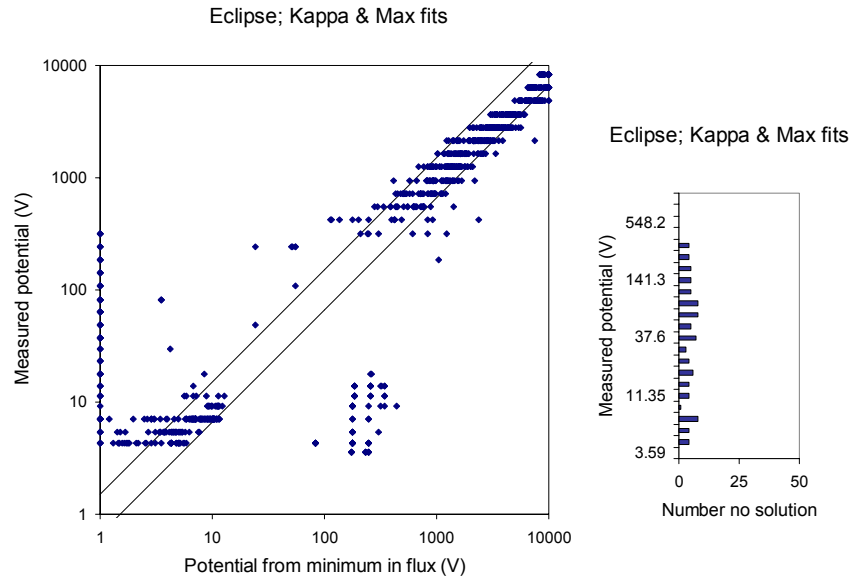
Figure 5. Measured potential computed from the minimum in the net charging flux, where the fluxes are computed from a Kappa fit to the electron flux and a Maxwellian fit to the ion flux.

Summary and Discussion

The LANL dataset has proven to be a powerful tool for the investigation of spacecraft surface charging. The flux spectra provide adequate resolution and accuracy for "postdiction" spacecraft surface charging calculations.

Using the measured flux spectra, we determined that for this spacecraft, computing the fluxes using a set of material properties for graphite carbon and a low-energy secondary electron escape fraction of 81%, gives computed potentials consistent with measured values. The estimated potential is within a factor of 1.5 of the measured potential for 66% of the data and within a factor of 3 for 87% of the data. While this approach is valid for any spacecraft in eclipse, where geometric effects are less important, the specific material properties and secondary electron escape fraction are spacecraft-specific quantities.

It is necessary to include all the current components–incident electrons and ions, secondary electrons, backscattered electrons, and (in sunlight) photoelectrons–to accurately "postdict" chassis potentials from measured flux spectra.

Potential "postdictions" using a Kappa distribution to fit the incident electron flux spectrum and a Maxwellian distribution to fit the incident ion flux spectrum give results similar to "post-

dictions" using the measured flux spectra directly. We expect better results would be obtained if additional intelligence in the low energy portion of the flux spectrum was added to the ion flux fitting procedure. While the specific material properties and secondary electron escape fraction are spacecraft-specific, the conclusion regarding the best functional forms to use for the environment are appropriate to all geosynchronous spacecraft.

The difference between a Maxwellian distribution and a Kappa distribution is in the tail of the distribution. The Kappa distribution falls off more slowly with energy. The difference between the accuracy of results computed using the two types of fits is consistent with earlier work by Katz et al.[5] in which it was shown that the form of the secondary yield in the high energy range is critical to the computation of spacecraft charging.

While this study has established that a Kappa distribution fit rather than a Maxwellian distribution fit to a known electron flux spectrum is preferred for spacecraft charging calculations, the question of the appropriate parameters to use for preflight predictions remains. A similar study using sunlit data and spacecraft geometric information would provide additional support for the results.

__Acknowledgments__

References

1. S.J. Bame, D.J. McComas, M.F. Thomsen, B.L. Barraclough, R.C. Elphic, J.P. Glore, and J.T. Gosling, Magnetospheric plasma analyzer for spacecraft with constrained resources, Rev Sci Instrum 64, p 1026, 1993.

2. M. F. Thomsen, D. J. McComas, G.D. Reeves, and L.A. Weiss, An observational test of the Tsyganenko (T89a) model of the magnetospheric field, JGR 101, p. 24827, 1996.

3. Purvis, C.K., H.B. Garrett, A.C. Whittlesey, and N.J. Stevens, Design Guidelines for Assessing and Controlling Spacecraft Charging Effects, NASA Technical Report Paper 2361, September 1984.

4. S.P. Christon, D.J. Williams, and D.G. Mitchell, L.A. Frank, C.Y. Huang, Spectral characteristics of plasma sheet ion and electron populations during undisturbed geomagnetic conditions, J. Geophys. Res. 94, A10, p 13,409, 1989.

5. I. Katz, M.J. Mandell, G.A. Jongeward, The importance of accurate secondary electron yields in modeling spacecraft charging, JGR, 91, p. 13739, 1986.